ELSEVIER

The structure of flame filaments in chaotic flows

I.Z. Kiss [a], J.H. Merkin [a,*], S.K. Scott [b], P.L. Simon [b], S. Kalliadasis [c], Z. Neufeld [d]

[a] *Department of Applied Mathematics, University of Leeds, Leeds LS2 9JT, UK*
[b] *Department of Chemistry, University of Leeds, Leeds LS2 9JT, UK*
[c] *Department of Chemical Engineering, University of Leeds, Leeds LS2 9JT, UK*
[d] *Department of Applied Mathematics and Theoretical Physics, University of Cambridge, Silver Street, Cambridge CB3 9EW, UK*

Abstract

The structure of flame filaments resulting from chaotic mixing within a combustion reaction is considered. The transverse profile of the filaments is investigated numerically and analytically based on a one-dimensional model that represents the effect of stirring as a convergent flow. The dependence of the steady solutions on the Damköhler number and Lewis number is treated in detail. It is found that, below a critical Damköhler number Da_{crit}, the flame is quenched by the flow. The quenching transition appears as a result of a saddle-node bifurcation where the stable steady filament solution collides with an unstable one. The shape of the steady solutions for the concentration and temperature profiles changes with the Lewis number and the value of Da_{crit} increases monotonically with the Lewis number. Properties of the solutions are studied analytically in the limit of large Damköhler number and for small and large Lewis number.
© 2002 Elsevier Science B.V. All rights reserved.

1. Introduction

Many chemical and biological processes take place within an imperfectly mixed environment, examples include the mixing of reactants within continuously fed or batch reactors [1] and in the spread of plankton blooms within oceanic currents [2,3]. In these situations the time-dependent fluid flow, within which the reactions are taking place, can lead to the chaotic transport of fluid elements [4–7], which become stretched into thin elongated filaments. This behaviour has been observed both experimentally by inserting dye droplets into the flow [8–12] and in numerical simulations [11,13].

In a two-dimensional system, a convergent and a divergent direction can be assigned to any point in the flow associated with the eigenvectors corresponding to the negative and positive Lyapunov exponents $-\lambda$ and λ of the chaotic advection [14,15]. These directions are, respectively, tangent to the stable and unstable foliations of the

---

* Corresponding author. Tel.: +44-113-343-5108; fax: +44-113-343-5090.
E-mail address: amtjhm@amsta.leeds.ac.uk (J.H. Merkin).

advection dynamics. Any advected material line tends to align along the unstable foliation in forward time, or along the stable foliation in backward time. Thus, the stirring process smoothes out the concentration of any advected tracer along the stretching direction, whilst enhancing concentration gradients in the convergent direction, producing a quasi-one-dimensional 'lamellar' structure.

This allows us to separate the original reaction–advection–diffusion problem along the (Lagrangian) stretching and converging directions. In the stretching direction any perturbation is spread by the advective transport. This is the dominant process in this case and is much faster than diffusion. In the convergent direction, however, all three processes of reaction, advection and diffusion are of equal importance and need to be considered together. Chemical reactions of the type $A + B \rightarrow P$ taking place in one-dimensional lamellar systems were first studied numerically by Muzzio and Ottino [16–18] and analytically by Sokolov and Blumen [19]. More recently, Clifford et al. [20,21] investigated the evolution of a two-step (competitive–consecutive) chemical reaction in lamellar systems.

For a spatially smooth velocity field the relative motion of nearby fluid elements can be approximated by linearising the velocity field along the path of a fluid particle. Thus, in the convergent direction fluid elements approach each other with a relative velocity proportional to their separation, $\delta v \sim -a(t)\delta r$, where the rate of convergence generally fluctuates in time along the trajectory. The average behaviour can be approximated by replacing $a(t)$ with its long time average given by λ, the Lyapunov exponent of the chaotic advection. In the context of autocatalytic type reactions it has been shown, that the resulting one-dimensional 'Lagrangian filament model' can be used to describe the mean transverse profiles of filaments that propagate along the divergent direction following the unstable foliation [22,23].

Fluid mixing has an important role in combustion [24–28]. Our main aim is to consider the effect of chaotic mixing within a combustion reaction, which we model as a first-order process converting a fuel C to an inert product P through the reaction

$$C \rightarrow P, \quad \text{rate} = ck(T) \tag{1}$$

with exothermicity q. T is the (absolute) temperature and c the concentration of reactant C. The temperature dependence of the reaction rate is given by an Arrhenius law with an ignition temperature T_i, namely

$$k(T) = \begin{cases} k_0 \exp\left(-\dfrac{E}{RT}\right) & \text{if } T > T_i, \\[2mm] 0 & \text{if } T \leq T_i, \end{cases} \tag{2}$$

where E and R are the activation energy and the universal gas constant and k_0 is the (constant) pre-exponential factor. Our reason for choosing this form for the rate law is to avoid the difficulties associated with the cold boundary problem. An alternative approach is, rather artificially, to set the ambient temperature to 0. The form given by (2) allows for a nonzero ambient temperature and the discontinuity in $k(T)$ does not lead to any problems provided T_i is kept small.

Here we are concerned with the structures of filaments that arise within the chaotic mixing and so, for present purposes, the nature of the time-dependent fluid flow is not important. This aspect will be described in a future paper [29] along with details of the resulting chaotic transport and reaction processes. This leads us to consider the equations for the filament structure

$$\rho C_p \left(\frac{\partial T}{\partial t} - \lambda x \frac{\partial T}{\partial x}\right) = \kappa \frac{\partial^2 T}{\partial x^2} + qck(T), \tag{3}$$

$$\frac{\partial c}{\partial t} - \lambda x \frac{\partial c}{\partial x} = D \frac{\partial^2 c}{\partial x^2} - ck(T) \tag{4}$$

on $-\infty < x < \infty$, $t > 0$. Here x measures distance transverse to the filament, t time and ρ the density, C_p the specific heat, κ and D are the thermal conductivity and diffusion coefficient, respectively.

The convective terms in Eqs. (3) and (4) can be interpreted as advection by a pure strain flow at a constant stretching rate $-\lambda$ ($\lambda > 0$) along the convergent direction. We can associate λ with the Lyapunov exponent of the chaotic advection. Equations similar to (3) and (4) were first proposed by Ranz [30] and have been considered previously for somewhat simpler chemical systems [19,20] including autocatalytic reactions [23] and excitable media [22], where their significance in determining the nature of the chaotic mixing is brought out. These previous studies considered only chemical systems with identical diffusivities for all species. An important new aspect investigated in this paper is the possibility of different diffusivities for heat and reactant, characteristic to the combustion process.

We apply the boundary conditions

$$T \to T_a, \qquad c \to c_0 \quad \text{as } |x| \to \infty \ (t > 0), \tag{5}$$

where T_a is the ambient temperature (we are assuming that $T_a < T_i$). For the time-dependent problem we initiate the reaction by applying a local temperature input (above T_i).

To make Eqs. (3) and (4) dimensionless, we introduce the variables

$$\bar{T} = \frac{T - T_a}{T_b - T_a}, \qquad \bar{c} = \frac{c}{c_0}, \qquad \bar{t} = \lambda t, \qquad \bar{x} = x\sqrt{\frac{\lambda}{D}}, \tag{6}$$

where T_b is the burnt temperature $T_b = T_a + (qc_0/\rho C_p)$. This leads to the equations, on dropping the bars for convenience,

$$\frac{\partial T}{\partial t} - x\frac{\partial T}{\partial x} = Le\frac{\partial^2 T}{\partial x^2} + Da\, cK(T), \tag{7}$$

$$\frac{\partial c}{\partial t} - x\frac{\partial c}{\partial x} = \frac{\partial^2 c}{\partial x^2} - Da\, cK(T), \tag{8}$$

where

$$Da = \frac{k_0}{\lambda}, \qquad Le = \frac{\kappa}{\rho C_p D}$$

are the Damköhler and Lewis numbers, respectively. The temperature dependence of the reaction (2) becomes

$$K(T) = \begin{cases} \exp\left(-\dfrac{1}{\epsilon((1-\beta)T + \beta)}\right) & \text{if } T > \bar{T}_i, \\ 0 & \text{if } T \le \bar{T}_i, \end{cases} \tag{9}$$

where

$$\epsilon = \frac{RT_b}{E}, \qquad \beta = \frac{T_a}{T_b}, \qquad \bar{T}_i = \frac{T_i - T_a}{T_b - T_a}.$$

The boundary conditions to be applied are that

$$T \to 0, \qquad c \to 1 \quad \text{as } |x| \to \infty. \tag{10}$$

The Damköhler number Da characterises the ratio between the advective and the chemical time-scales. Large Da corresponds to slow stirring or equivalently fast chemical reaction and vice versa. This, together with the Lewis number Le, are our main bifurcation parameters.

We start by considering the possible steady-state solutions to Eqs. (7) and (8) satisfying boundary conditions (10).

2. Steady states

Here we consider the steady equations

$$Le\, T'' + xT' + Da\, cK(T) = 0, \qquad c'' + xc' - Da\, cK(T) = 0, \tag{11}$$

where $K(T)$ is given by (9) and where primes denote differentiation with respect to x. We look for symmetric solutions, applying the boundary conditions

$$T'(0) = c'(0) = 0, \qquad T \to 0, \qquad c \to 1 \ \text{as}\, x \to \infty. \tag{12}$$

When $Le = 1$ we can combine Eqs. (11) to eliminate the reaction terms. Integrating the resulting equation and applying (12) gives $T + c \equiv 1$ and then

$$T'' + xT' + Da(1 - T)K(T) = 0 \tag{13}$$

again subject to (12).

Eqs. (11) or (13) were solved numerically using a standard NAG library routine for integrating boundary-value problems. The outer boundary conditions were applied at a large value of x allowing them to be satisfied with sufficient accuracy. This value depended on the width of the filament which, in turn, depended on both the Lewis and Damköhler numbers. The numerical integrations were found to be insensitive to point where the outer conditions were taken. The results are presented in Fig. 1, where we plot T profiles for $Le = 1$ (Fig. 1a) and both T and c profiles for $Le = 0.1$ (Fig. 1b) and $Le = 10$ (Fig. 1c) for representative values of Da ($\epsilon = 1.0$, $\beta = 0.1$, $\bar{T}_\text{i} = 0.001$). In these figures the broken lines represent temporally unstable solutions (see below). As Da is increased for the stable solutions (full lines) the width of the filament increases with the temperature reaching a constant value within the central part of the filament. This central temperature quickly reaches a value of unity for $Le = 1.0$, whereas, for $Le = 10.0$, it slowly approaches this value from below as Da increases. The reactant C is fully consumed in this central region of the filament. For $Le = 0.1$, the reaction zone is much thinner than for the other two cases. Much higher temperatures can be achieved within the filament, though these reduce to unity, now from above, as Da is increased. In all cases the unstable solutions (broken lines) reduce in both magnitude and extent as Da increases.

To see how the solutions change as a given parameter is varied, we need some measure of the solution. The profiles shown in Fig. 1 suggest that the integrated quantity

$$I_T = \int_0^\infty T(x)\, \mathrm{d}x \tag{14}$$

is a suitable measure. Note that, if we add Eqs. (11), integrate the resulting equation and apply boundary conditions (12), we find that $I_T = \int_0^\infty T(x)\, \mathrm{d}x = \int_0^\infty (1 - c(x))\, \mathrm{d}x$. Graphs of I_T against Da are shown in Fig. 2 (for $Le = 0.1, 1, 10$). The figure shows that there is a critical value of the Damköhler number, Da_crit, with a saddle-node bifurcation at Da_crit giving two solutions for $Da > Da_\text{crit}$ and no solutions for $Da < Da_\text{crit}$, apart from the trivial uniform solution, $C(x) = 1$, $T(x) = 0$, corresponding to the extinction of the flame. Thus, the transition at Da_crit can be interpreted as a quenching transition when the burning of the fuel is not sufficiently fast to compensate for the diluting effect of the stirring, which tends to reduce the temperature of the filament. I_T increases with Da on the upper solution branch and decreases on the lower branch. This effect can also be seen in the profiles shown in

Fig. 1. (a) Temperature T profiles for $Le = 1$ (Da takes values from 6.965 to 100 for the stable solutions and from 7 to 75 for the unstable solutions). Temperature T and concentration c profiles for (b) $Le = 0.1$ (Da takes values from 5 to 70 for the stable solutions and from 6 to 20 for the unstable solutions) and (c) $Le = 10$ (Da takes values from 8.5 to 50 for the stable solutions and from 8.7 to 50 for the unstable solutions) ($\epsilon = 1.0$, $\beta = 0.1$, $\bar{T}_\text{i} = 0.001$). The broken lines represent temporally unstable solutions.
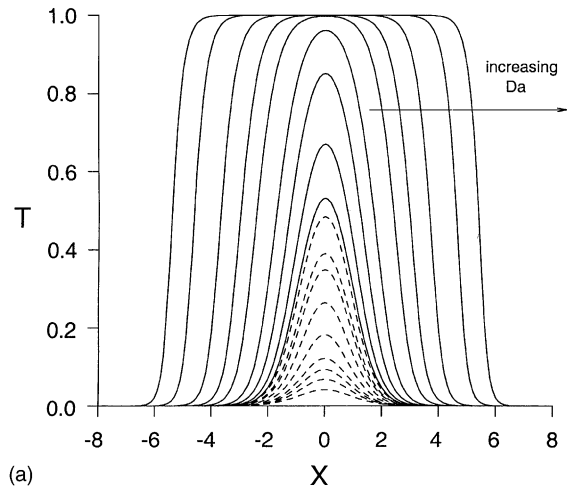
(a)
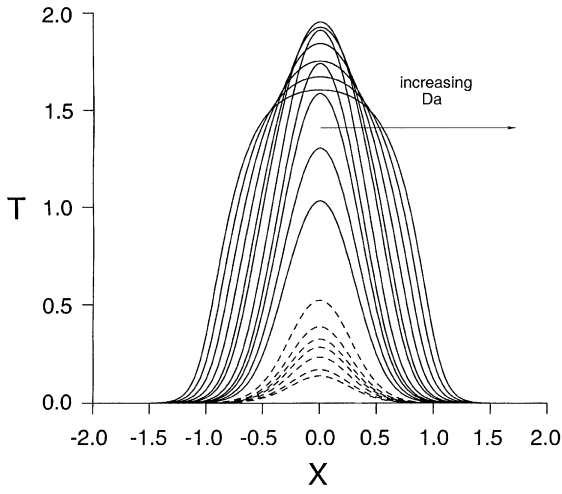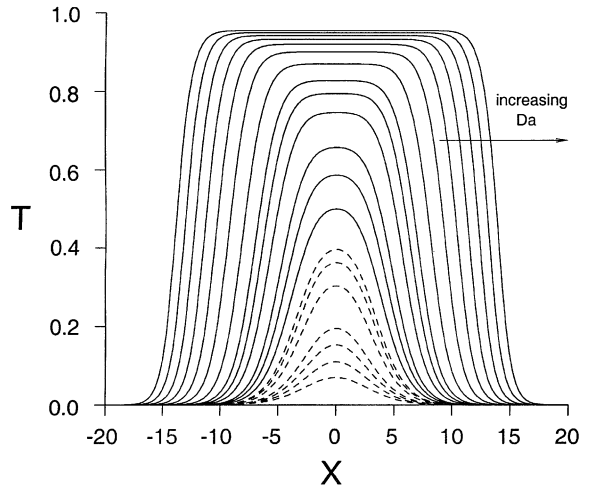
(b)   (c)
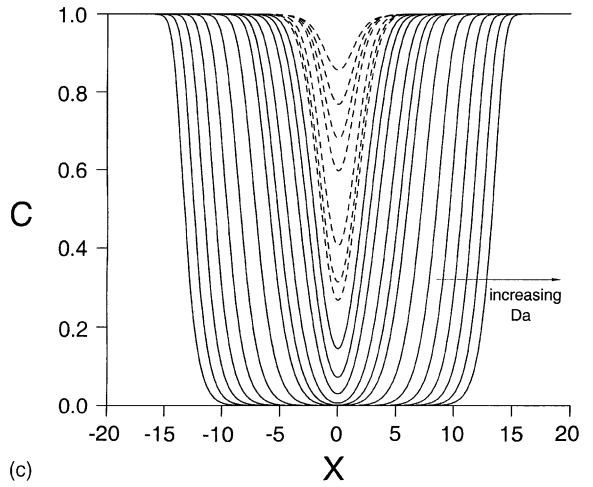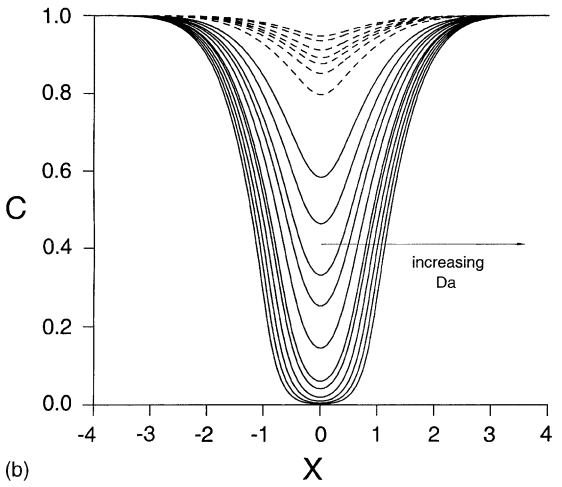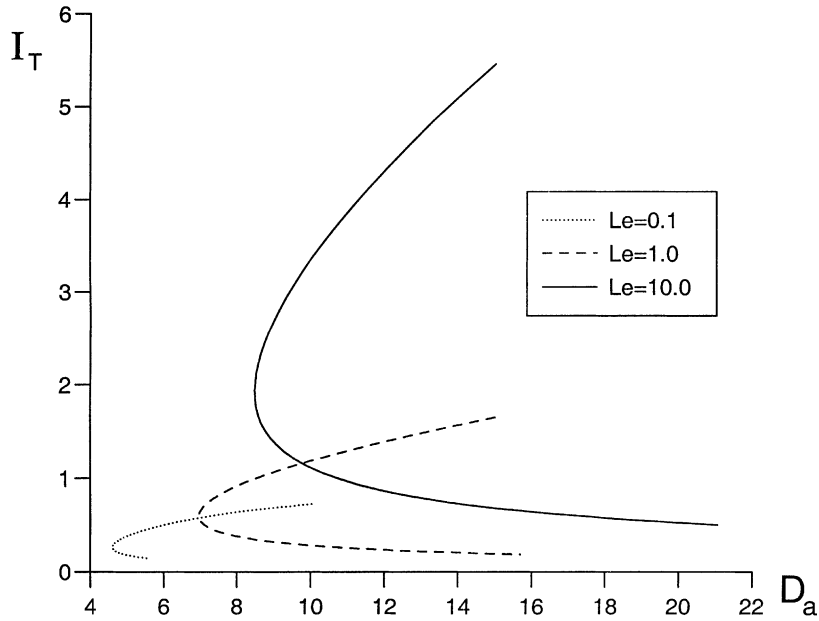
Fig. 2. Graphs of I_T (defined by (14)) against Da for $Le = 0.1, 1, 10$ ($\epsilon = 1.0, \beta = 0.1, \bar{T}_i = 0.001$). The lower branch solutions are temporally unstable.

Fig. 1. Note that the value of Da_{crit} appears to increase with Le. We also note, that the possibility of quenching a flame by a sufficiently strong shear flow has been shown recently in a rigorous mathematical study by Constantin et al. [28].

We can compute Da_{crit} as a function of the other parameters through looking for a nontrivial solution to the homogeneous linear equations that are obtained by making a small perturbation to the solution of Eqs. (11) (or (13)). This point will be made clearer when we discuss the stability of the steady states in the next section. A graph of Da_{crit} against Le computed in this way is shown in Fig. 3 (for $\epsilon = 1.0, \beta = 0.1, \bar{T}_i = 0.001$). The figure shows that Da_{crit} approaches a finite value (approximately 8.5 for this case) as $Le \to \infty$ and approaches a nonzero value as $Le \to 0$.

The graphs shown in Figs. 1–3 show different forms of behaviour depending on whether Le is small or large. There is also a distinctive structure of the reaction zone when Da is large and it is this limit that we now consider.

2.1. Solution for large Da

Here we describe how the upper branch (stable) solutions behave for Da large. The form of the graphs shown in Fig. 1 suggest that, for $Da \gg 1$, the profiles have two regions of constant temperature and concentration. There is a central (fully reacted) region where $T = T_c$, $c = 0$ and an outer (unreacted region) where $T = 0$, $c = 1$. There then must be a reaction zone which joins these two regions and which smoothes out the discontinuities in temperature and concentration. To determine the structure of this reaction zone we assume that it is centred on $x = x_0(Da)$. We then put

$$X = Da^{1/2}(x - x_0) \tag{15}$$

and look for a solution by expanding
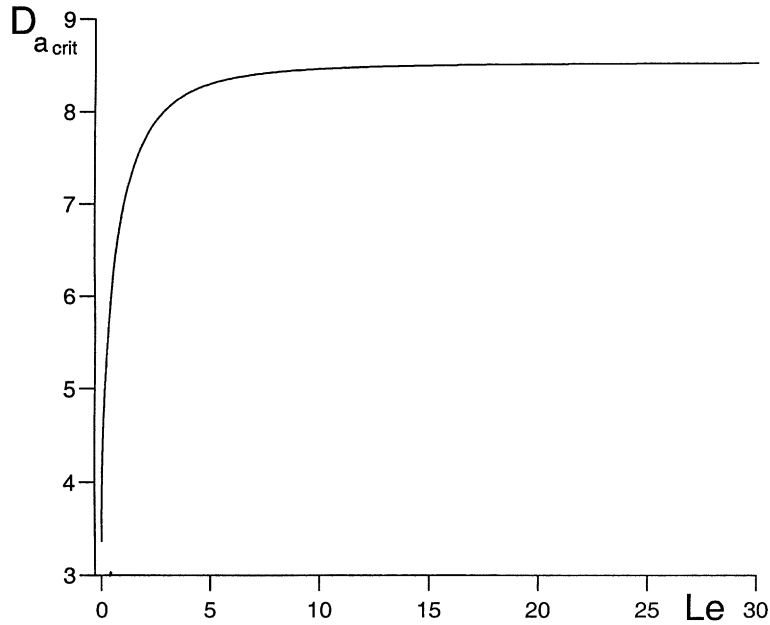
Fig. 3. A plot of Da_{crit} against Le ($\epsilon = 1.0$, $\beta = 0.1$, $\bar{T}_i = 0.001$).

$$T(X; Da) = T_0(X) + Da^{-1}T_1(X) + \cdots, \qquad c(X; Da) = c_0(X) + Da^{-1}c_1(X) + \cdots,$$

$$T_c(Da) = T_c^{(0)} + Da^{-1}T_c^{(1)} + \cdots. \tag{16}$$

A consideration of the resulting equations suggests that x_0 is of $O(Da^{1/2})$. This suggests that we put

$$x_0(Da) = Da^{1/2}(a_0 + a_1 Da^{-1} + \cdots), \quad Da \gg 1, \tag{17}$$

where the a_i are constants to be determined.

The equations at leading order are then

$$Le\, T_0'' + a_0 T_0' + c_0 K(T_0) = 0, \qquad c_0'' + a_0 c_0' - c_0 K(T_0) = 0 \tag{18}$$

subject to the matching conditions

$$T_0 \to 0, \qquad c_0 \to 1 \quad \text{as } X \to \infty, \qquad T_0 \to T_c^{(0)}, \qquad c_0 \to 0 \quad \text{as } X \to -\infty. \tag{19}$$

Primes now denote differentiation with respect to X. If we add Eqs. (18), integrate and apply the boundary conditions as $X \to \infty$ we obtain the equation

$$Le\, T_0' + a_0 T_0 + c_0' + a_0 c_0 = a_0. \tag{20}$$

If we now let $X \to -\infty$ in Eq. (20), we find, on using (19), that

$$T_c^{(0)} = 1. \tag{21}$$

This result shows, from (6), that the central temperature within a filament is the burnt temperature T_b for large Damköhler numbers.

It is the solution to the first equation of (18) and (20) subject to (19) and using (21) that determines a_0. This boundary-value problem was solved numerically in a way similar to that used for determining the general filament
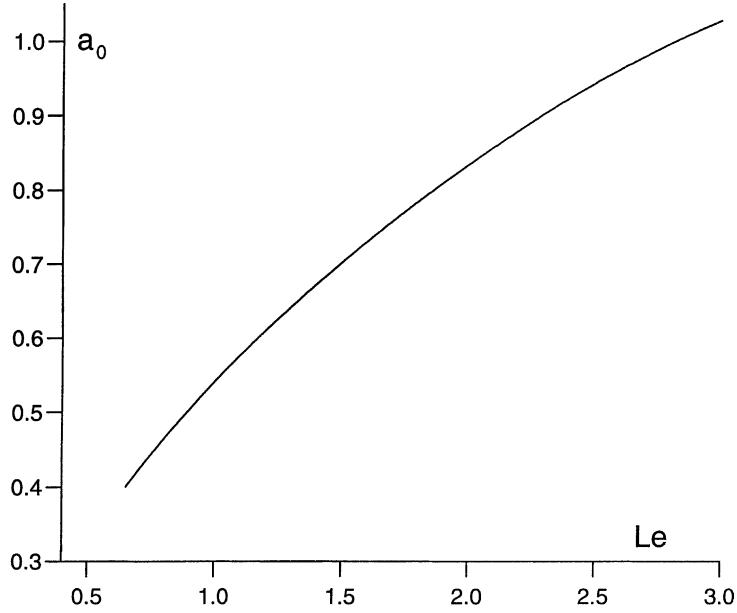
Fig. 4. The solution for $Da \gg 1$; a_0, the thickness of the central, fully reacted region, plotted against Le ($\epsilon = 1.0$, $\beta = 0.1$, $\bar{T}_i = 0.001$).

solutions. A graph of a_0 against Le is shown in Fig. 4 for $\epsilon = 1.0$, $\beta = 0.1$, $\bar{T}_i = 0.001$. The figure shows that a_0, the position of the reaction front for large Da, increases with Le, in line with the profiles shown in Fig. 1.

We now consider the equations at $O(Da^{-1})$. We find, as before, that we can add these equations to eliminate the reaction terms to obtain

$$Le\, T_1'' + a_0 T_1' + (X + a_1)T_0' + c_1'' + a_0 c_1' + (X + a_1)c_0' = 0. \tag{22}$$

The boundary conditions to be applied are that

$$T_1 \to T_c^{(1)} \qquad c_1 \to 0 \quad \text{as } X \to -\infty, \qquad T_1 \to 0 \qquad c_1 \to 0 \quad \text{as } X \to \infty. \tag{23}$$

If we integrate Eq. (22) and apply boundary conditions (19) and (23) we obtain, on using (21)

$$a_0 T_c^{(1)} = \int_{-\infty}^{\infty} (1 - c_0 - T_0)\, dX. \tag{24}$$

The integral in (24) can then be evaluated as $(1 - Le)/a_0$ by integrating equation (20). Thus we have

$$T_c^{(1)} = \frac{1 - Le}{a_0^2} \quad \text{with } T_c \sim 1 + Da^{-1}\left(\frac{1 - Le}{a_0^2}\right) \cdots \quad \text{as } Da \to \infty. \tag{25}$$

Expression (25) gives $T_c^{(1)} = 0$ when $Le = 1$ and shows why, in the central region, the burnt temperature is approached from below for $Le > 1$ and from above for $Le < 1$.

2.2. Solution for small Le

Here we obtain a solution to Eqs. (11) valid for $Le \ll 1$. We assume that Da is of $O(1)$ and start by making the transformation $\xi = Le^{-1/2}x$. This leads to the equations

$$T'' + \xi T' + Da\, cK(T) = 0, \qquad c'' + Le(\xi c' - Da\, cK(T)) = 0 \tag{26}$$

still subject to (12), where primes now denote differentiation with respect to ξ. Eq. (26) suggest looking for a solution by expanding in powers of Le. However, we find that this is not sufficient and we need to expand in powers of $Le^{1/2}$, namely

$$T = T_0 + Le^{1/2}\, T_1 + Le\, T_2 + \cdots, \qquad c = c_0 + Le^{1/2}\, c_1 + Le\, c_2 + \cdots. \tag{27}$$

At leading order $c_0'' = 0$ from which it follows that

$$c_0 \equiv 1 \tag{28}$$

and then

$$T_0'' + \xi T_0' + Da\, K(T_0) = 0. \tag{29}$$

The numerical solution of Eq. (29), subject to (12), shows that it has a similar structure to the results shown in Figs. 1 and 2. From the co-ordinate transformation $I_T = Le^{1/2}\, \bar{I}_T$ where $\bar{I}_T = \int_0^\infty T_0(\xi)\, \mathrm{d}\xi$. A graph of $\bar{I}_T$ against Da is shown in Fig. 5. The main point to note about this figure is the existence of a critical Damköhler number $Da_{\mathrm{crit}} = 3.0136$ with two solution branches for $Da > Da_{\mathrm{crit}}$. This is the limiting value of Da_{crit} at $Le = 0$ in Fig. 3. Note that the value of I_T at Da_{crit} decreases with Le with $I_T \sim 1.530 Le^{1/2}$ as $Le \to 0$.

At $\mathrm{O}(Le^{1/2})$ we have $c_1'' = 0$. Hence $c_1 = b_1$, where b_1 is a constant to be determined. At $\mathrm{O}(Le)$ we then have

$$c_2'' = Da\, K(T_0), \qquad c_2'(0) = 0. \tag{30}$$

We can integrate Eq. (30) and using the result obtained from Eq. (29) that $Da \int_0^\infty K(T_0)\, \mathrm{d}\xi = \bar{I}_T$, we have that

$$c_2 \sim \bar{I}_T \xi + b_2 \quad \text{as } \xi \to \infty \tag{31}$$
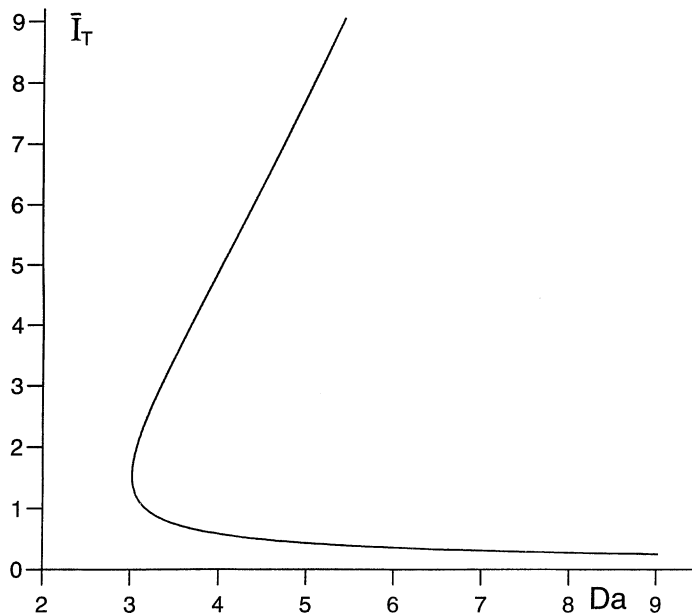


Fig. 5. The solution for $Le \ll 1$; $\bar{I}_T$, obtained from the numerical solution of Eq. (29), plotted against Da ($\epsilon = 1.0$, $\beta = 0.1$, $\bar{T}_{\mathrm{i}} = 0.001$).

for some further constant b_2. A consideration of the equations for the T_j ($j \geq 1$) in expansion (27) shows that they can be solved so as to satisfy the outer boundary condition.

Expression (31) shows that we require an outer region in which $T \equiv 0$, in which x is now the independent variable and $c = 1 + Le^{1/2}\bar{c}$. At leading order we obtain

$$\bar{c}'' + x\bar{c}' = 0, \qquad \bar{c} \sim b_1 + \bar{I}_T x + \cdots \quad \text{as} \ x \to 0, \qquad \bar{c} \to 0 \quad \text{as} \ x \to \infty. \tag{32}$$

The required solution is

$$\bar{c} = b_1 \sqrt{\frac{2}{\pi}} \int_x^\infty \exp\left(-\frac{s^2}{2}\right) \, \mathrm{d}s = b_1 \left[1 - \mathrm{erf}\left(\frac{x}{\sqrt{2}}\right)\right]. \tag{33}$$

Using the matching condition for x small then gives $b_1 = -\bar{I}_T \sqrt{\pi/2}$. The concentration at the centre of the filament is then

$$c(0) = 1 - Le^{1/2} \bar{I}_T (Da) \sqrt{\frac{\pi}{2}} + \cdots \quad \text{as} \ Le \to 0. \tag{34}$$

We can now see why the terms of $Le^{1/2}$ are required in the expansion (27). Without these terms b_1 would effectively be zero, the solution to Eq. (30) at O(Le) would be the same and again would not satisfy the outer boundary condition ((31) still holds). An outer region would still be needed and be given by (32) though with $b_1 = 0$. A solution to this problem cannot be obtained along the lines given by (33).

2.3. Solution for large Le

The structure of the solution for $Le \gg 1$ is illustrated in Fig. 6 for $Le = 10^3$ and $Da = 12.0$ ($\epsilon = 1.0$, $\beta = 0.1$, $\bar{T}_i = 0.001$). The graph shows that there is an inner region around $x = 0$ where c is very small and T is approximately
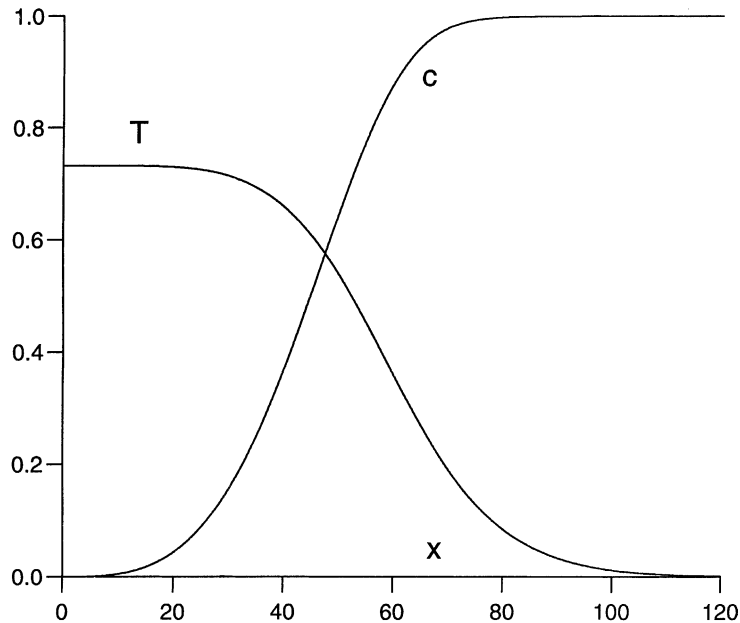

Fig. 6. The solution for large Le; concentration c and temperature T profiles for $Le = 10^3$, $Da = 12.0$ ($\epsilon = 1.0$, $\beta = 0.1$, $\bar{T}_i = 0.001$).

a constant. We start our solution for Le large in this inner region. We leave x unscaled and look for a solution of Eq. (11) by expanding

$$T(x; Le) = T_c + Le^{-(1+m)}T_1(x)\dots, \qquad c(x; Le) = Le^{-m}c_1(x) + \dots, \tag{35}$$

where $m\ (> 0)$ and $T_c\ (\neq 0)$ are to be determined. The equation for c_1 is

$$c_1'' + xc_1' - \alpha c_1 = 0, \qquad c_1'(0) = 0, \tag{36}$$

where $\alpha = Da\,K(T_c)$ is a constant. Eq. (36) can be solved in terms of confluent hypergeometric functions [31] as

$$c_1(x) = A_0 \exp\left(-\frac{x^2}{2}\right) {}_1F_1\left(\frac{\alpha+1}{2}; \frac{1}{2}; \frac{x^2}{2}\right) \tag{37}$$

for some constant A_0. From (37) it follows that

$$c_1(x) \sim \frac{A_0\sqrt{\pi}}{((\alpha-1)/2)!\,2^{\alpha/2}}x^\alpha(1 + \cdots) \quad \text{as } x \to \infty. \tag{38}$$

The equation for $T_1(x)$ is $T_1''(x) = -\alpha c_1(x)$ which can be integrated to give

$$T_1(x) = -\frac{\alpha A_0}{(\alpha+2)}\exp\left(-\frac{x^2}{x}\right) {}_1F_1\left(\frac{\alpha+3}{2}; \frac{1}{2}; \frac{x^2}{2}\right) + B_1 \tag{39}$$

for some further constant B_1. From (39)

$$T_1(x) \sim -\frac{A_0\alpha\sqrt{\pi}}{2(\alpha+2)((\alpha+1)/2)!\,2^{\alpha/2}}x^{\alpha+1}(1 + \cdots) \quad \text{as } x \to \infty. \tag{40}$$

An outer region is required to satisfy the outer boundary conditions. The form of Eq. (11) suggests that the appropriate scaling for this outer region is $\xi = Le^{-1/2}x$ with c and T both of O(1). Applying this scaling in expressions (38) and (40) shows that we should take $m = \alpha/2$. With this, the problem for the outer region is, at leading order

$$T'' + \xi T' + Da\,K(T) = 0, \qquad \xi c' - Da\,K(T) = 0 \tag{41}$$

(primes denote differentiation with respect to ξ) subject to

$$c \sim \bar{A}_0\xi^\alpha + \cdots, \quad T \sim T_c - \frac{\alpha \bar{A}_0}{(\alpha+2)(\alpha+1)}\xi^{\alpha+2} + \cdots \quad \text{as } \xi \to 0, \ c \to 1, \ T \to 0 \text{ as } \xi \to \infty, \tag{42}$$

where $\bar{A}_0 = A_0\sqrt{\pi}/2^{\alpha/2}((\alpha-1)/2)!$.

The problem given by (41) and (42) has to be solved numerically and it is this solution that determines T_c (and $\bar{A}_0$). The results are shown in Fig. 7a, where we plot $\bar{I}_T = \int_0^\infty T(\xi)\,\mathrm{d}\xi$ against Da (for $\epsilon = 1.0$, $\beta = 0.1$, $\bar{T}_i = 0.001$). Note that $I_T = Le^{1/2}\bar{I}_T$. The graph shows that there is a critical Damköhler number $Da_{crit} = 8.503$, with two solutions for $Da > Da_{crit}$. This value for Da_{crit} is the limiting value for large Le seen in Fig. 3. The numerical solution gives T_c and hence the exponent $m = (1/2)\,Da\exp(-(1/\epsilon((1-\beta)T_c + \beta)))$ for expansion (35) in the inner region. Graphs of m and T_c are shown in Fig. 7b.

3. Stability of the steady states

To determine the stability of the steady states, we make a perturbation of the form

$$T(x, t) = T_s(x) + \mathrm{e}^{\omega t}T_1(x), \qquad c(x, t) = c_s(x) + \mathrm{e}^{\omega t}c_1(x), \tag{43}$$
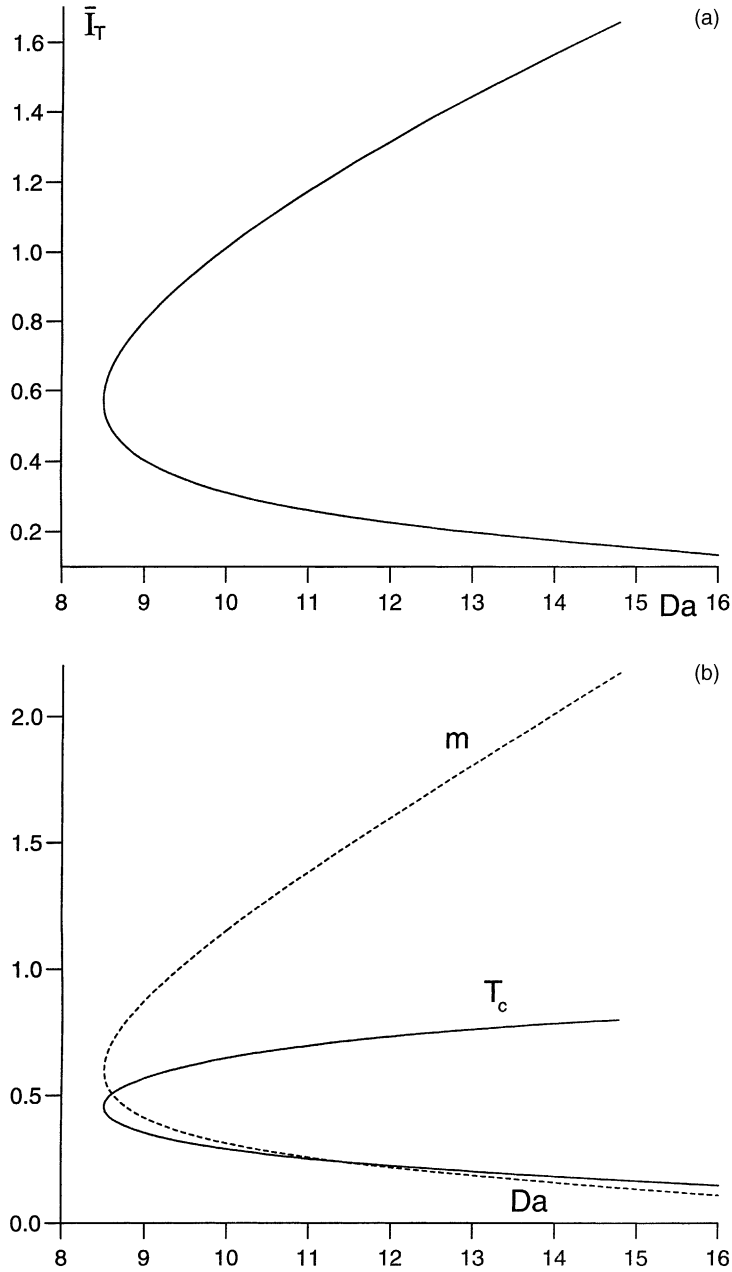
Fig. 7. The solution for large Le; (a) $\bar{I}_T$, (b) the central temperature T_c (full line) and the exponent m (broken line) for the inner region expansion (35) plotted against Da ($\epsilon = 1.0$, $\beta = 0.1$, $\bar{T}_i = 0.001$).

where T_s and c_s are the steady states (solutions of Eqs. (11) and (12)) and T_1 and c_1 are small. We must allow for the possibility that ω and T_1, c_1 could be complex. Substituting (43) into Eqs. (7) and (8) and linearizing gives

$$Le\,T_1'' + xT_1' + Da(c_1 K(T_s) + T_1 c_s K'(T_s)) - \omega T_1 = 0,$$
$$c_1'' + xc_1' - Da(c_1 K(T_s) + T_1 c_s K'(T_s)) - \omega c_1 = 0 \tag{44}$$
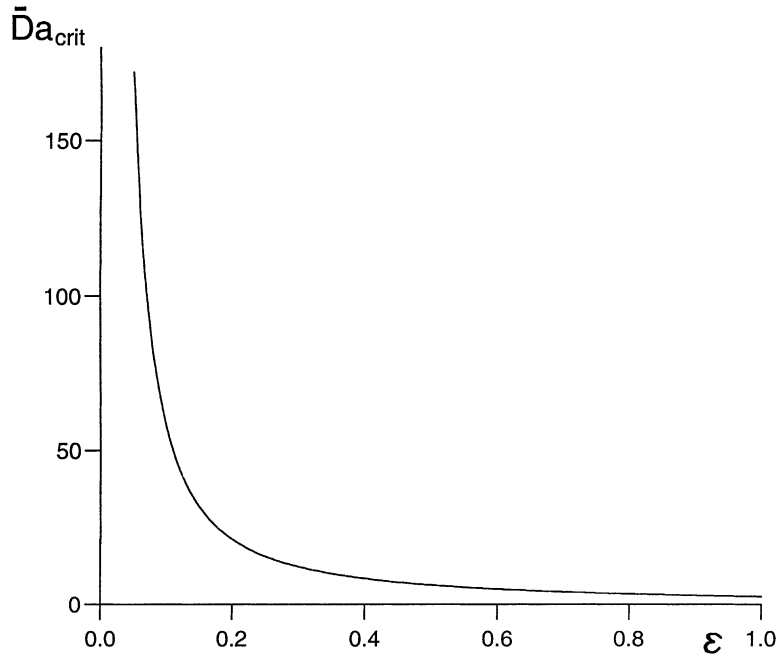
Fig. 8. A plot of $\overline{Da}_{\mathrm{crit}}$ against ϵ ($\overline{Da}_{\mathrm{crit}} = \mathrm{e}^{-1/\epsilon} Da_{\mathrm{crit}}$) for $Le = 1.0$, $\beta = 0.1$ ($\bar{T}_{\mathrm{i}} = 0.001$).

subject to

$$T_1'(0) = c_1'(0) = 0, \qquad T_1 \to 0, \qquad c_1 \to 0 \quad \text{as } x \to \infty. \tag{45}$$

Eqs. (44) and (45) are a homogeneous problem for the eigenvalue ω and to force a nontrivial solution in the numerical integrations we also apply the condition $T_1(0) = 1$.

The turning points in the I_T–Da curves (see Figs. 2, 5 and 7) correspond to saddle-node bifurcations, i.e. to points where ω has a real zero. Thus solving Eqs. (44) and (45) with $\omega = 0$ (and regarding Da as an unknown parameter) determines the value of Da at the saddle-node bifurcation, i.e. determines Da_{crit}. This was the procedure that was used to determine the values of Da_{crit} shown in Fig. 3. We can use this procedure to examine how Da_{crit} varies with the other parameters. We considered how Da_{crit} varied with ϵ. To do so we needed to think about the way in which we defined our Damköhler number. Our form uses k_0 for the reaction rate, perhaps a more suitable form is to use the reaction rate at the burnt gas temperature T_b to define a Damköhler number $\overline{Da}$, related to our choice by $\overline{Da} = \mathrm{e}^{-1/\epsilon} Da$. This change is not particularly significant for the larger values of ϵ that we used ($\epsilon \simeq 1$) but can be significant for smaller values of ϵ. In Fig. 8 we plot $\overline{Da}_{\mathrm{crit}}$ against ϵ for $Le = 1.0$, $\beta = 0.1$ (and $\bar{T}_{\mathrm{i}} = 0.001$). The graph shows that we can have nontrivial solutions even for small values of ϵ though relatively large values of ϵ are required to have reasonable values for $\overline{Da}_{\mathrm{crit}}$. For smaller values of ϵ (ϵ less than about 0.3) the values of $\overline{Da}_{\mathrm{crit}}$ increase very rapidly.

We solved Eqs. (44) and (45) numerically for a range of values of Le, varying Da. In all cases we found that the lower solution branch was unstable, in fact on this branch ω was real with $\omega > 0$. The upper branch solutions were found to be stable in all the cases considered. Generally, we found ω to be real and negative, though for high values of Le ($Le \sim 10^3$) we found that ω could become complex though always had $Re(\omega) < 0$. We were unable to locate any parameter values at which the solution became unstable (and oscillatory) through a Hopf bifurcation at $Re(\omega) = 0$. These conclusions were confirmed by numerical integrations of the initial-value problem (7), (8)

and (10). These showed that a threshold temperature input was necessary to generate a nontrivial solution and that, when this was applied, the corresponding upper branch solution was approached for t large when $Da > Da_{\mathrm{crit}}$. For $Da < Da_{\mathrm{crit}}$ the numerical solution returned to the initial state and the reaction ceased as t increased for all inputs.

4. Conclusion

The main feature to emerge from our discussion is the existence of a critical Damköhler number Da_{crit}. An important aspect of our kinetic model (1) and (2) in the reaction–diffusion context is that any localized temperature input has to be above some threshold value if spatial or statiotemporal structures are to be sustained at large times. The effect of the mixing by the flow, seen in our model (3) and (4) through the steady converging flow λx, is to remove the heat from where it is generated by the exothermic reaction. This has the effect of increasing the threshold input needed for steady structures to form at large times. Thus, for small values of the Damköhler number, mixing is too strong, the heat generated by the reaction is dissipated, the reaction cannot be sustained and the system returns to its original state. This means that relatively large values of the Damköhler number are required for nontrivial states to form within the filaments. This appears at a critical value Da_{crit} of the Damköhler number where there is a jump from the totally quenched state ($Da < Da_{\mathrm{crit}}$) to a fully developed state ($Da > Da_{\mathrm{crit}}$). Thus the values of Da_{crit} found in the present study are an important guide in determining where sustained combustion will arise in the more general flow problem [29].

We found that Da_{crit} is not particularly sensitive to the Lewis number (for the values of the other parameters considered), see Fig. 3, increasing from about 3 if Le is put to 0 and approaching a limit of about 8.5 for large values of Le. However, the resulting temperature and concentration profiles are strongly dependent on both Da and Le. For large values of Da a central, fully reacted core develops which is separated from the outer conditions by a relatively thin reaction zone. In this case combustion effects are spread out over a wide area of the filament. A similar situation arises for large values of the Lewis number. Here the influence of heat conduction is very much stronger than the diffusion of the reactant. The effect is to increase the spread of the reaction region to $\mathrm{O}(Le^{1/2})$, with a thinner inner region of constant temperature T_{c} somewhat less than the burnt gas temperature, see Figs. 6 and 7b. For small values of the Lewis number the reaction region becomes much thinner, large temperatures can be achieved (relative to the burnt gas temperature) and only small amounts of fuel are consumed.

Criticality is an inherent part of the system and appears to be present for all values of the parameters associated with the Arrhenius kinetics. To get 'reasonable' values for Da_{crit} requires that ϵ be relatively large (Fig. 8), which can be regarded as corresponding to smaller activation energies. This is in contrast to other combustion problems where criticality is seen only for the higher activation energies and disappears (sometimes through a hysteresis bifurcation) at a given activation energy. Finally, we note that we found only stable steady structures when $Da > Da_{\mathrm{crit}}$. We found no further bifurcations to oscillatory behaviour.

Finally, we note that the simple one-dimensional model (3) and (4) considered here is a somewhat idealised model of the full advection–reaction–diffusion problem in which the effects of fluctuations of the stretching rate, curvature of the filaments, interactions between filaments etc. are neglected. Such effects, however, may play an important role in certain situations and deserve further investigations.

Acknowledgements

References

[1] I.R. Epstein, The consequences of imperfect mixing in autocatalytic chemical and biological systems, Nature 374 (1995) 321–327.

[2] R. Abraham, C.S. Law, P.W. Boyd, S.J. Lavender, M.T. Maldonado, A.R. Bowie, Importance of stirring in the development of an iron-fertilized phytoplankton bloom, Nature 407 (2000) 727–730.

[3] Z. Neufeld, P.H. Haynes, V. Garcon, J. Sudre, Ocean fertilization experiments may initiate large-scale phytoplankton bloom, Geophys. Res. Lett. 29 10.1029/2001GL013677, 2002.

[4] H. Aref, Stirring by chaotic advection, J. Fluid Mech. 143 (1984) 1–21.

[5] J.M. Ottino, The Kinematics of Mixing: Stretching, Chaos and Transport, Cambridge University Press, Cambridge, 1989.

[6] J.M. Ottino, Mixing, chaotic advection and turbulence, Annu. Rev. Fluid Mech. 22 (1990) 207–253.

[7] T.H. Solomon, J.P. Gollub, Chaotic particle transport in time-dependent Rayleigh–Bénard convection, Phys. Rev. E 38 (1988) 6280–6286.

[8] J. Chaiken, R. Chevray, M. Tabor, Q.M. Tan, Experimental study of Lagrangian turbulence in a Stokes flow, Proc. R. Soc. Lond. A 408 (1986) 165–174.

[9] W.L. Chien, H. Rising, J.M. Ottino, Laminar mixing and chaotic mixing in several cavity flows, J. Fluid Mech. 170 (1986) 355–377.

[10] J.M. Ottino, C.W. Leong, H. Rising, P.D. Swanson, Morphological structures produced by mixing in chaotic flows, Nature 333 (1988) 419–425.

[11] S.C. Jana, G. Metcalfe, J.M. Ottino, Experimental and computational studies of mixing in complex Stokes flows: the vortex mixing flow and multicellular cavity flows, J. Fluid Mech. 269 (1994) 199–246.

[12] D. Rothstein, E. Henry, J.P. Gollub, Persistent patterns in transient chaotic fluid mixing, Nature 401 (1999) 770–772.

[13] M.M. Alvarez, F.J. Muzzio, S. Cerbelli, A. Adrover, M. Giona, Self-similar structure of intermaterial boundaries in chaotic flows, Phys. Rev. Lett. 81 (1998) 3395–3398.

[14] M. Giona, A. Adrover, F.J. Muzzio, S. Cerbelli, M. Alvarez, The geometry of mixing in time-periodic chaotic flows. I. Asymptotic directionality in physically realizable flows and global invariant properties, Physica D 132 (1999) 298–324.

[15] F. Városi, T.M. Antonsen, E. Ott, The spectrum of fractal dimensions of passively convected scalar gradients in chaotic fluid flows, Phys. Fluids A 3 (1991) 1017–1028.

[16] F.J. Muzzio, J.M. Ottino, Evolution of a lamellar system with diffusion and reaction: a scaling approach, Phys. Rev. Lett. 63 (1989) 47–50.

[17] F.J. Muzzio, J.M. Ottino, Dynamics of a lamellar system with diffusion and reaction: scaling analysis and global kinetics, Phys. Rev. A 40 (1989) 7182–7192.

[18] F.J. Muzzio, J.M. Ottino, Diffusion and reaction in a lamellar system: self-similarity with finite rates of reaction, Phys. Rev. A 42 (1990) 5873–5884.

[19] I.M. Sokolov, A. Blumen, Mixing effects in the $A + B$ reaction–diffusion scheme, Phys. Rev. Lett. 66 (1991) 1942–1945.

[20] M.J. Clifford, S.M. Cox, E.P.L. Roberts, Lamellar modelling of reaction, diffusion and mixing in a two-dimensional flow, Chem. Eng. J. 71 (1998) 49–56.

[21] M.J. Clifford, S.M. Cox, E.P.L. Roberts, Reaction and diffusion in a lamellar structure: the effect of the lamellar arrangement upon yield, Physica A 262 (1999) 294–306.

[22] Z. Neufeld, Excitable media in a chaotic flow, Phys. Rev. Lett. 87 (2001) 108301–108304.

[23] Z. Neufeld, P.H. Haynes, T. Tél, Chaotic mixing induced transitions in reaction–diffusion systems, Chaos 12 (2002) 426–438.

[24] N. Peters, Turbulent Combustion, Cambridge University Press, Cambridge, 2000.

[25] P. Constantin, A. Kiselev, A. Oberman, L. Ryzhik, Bulk burning rate in passive-reactive diffusion, Arch. Rational Mech. 154 (2000) 53–91.

[26] M. Abel, A. Celani, D. Vergni, A. Vulpiani, Front propagation in laminar flows, Phys. Rev. E 64 (2001) 46307.

[27] A. Kiselev, L. Ryzhik, Enhancement of the travelling front speeds in reaction–diffusion equations with advection, Ann. I.H. Poincaré 18 (2001) 309–358.

[28] P. Constantin, A. Kiselev, L. Rhyzik, Quenching of flames by fluid advection, Comm. Pure Appl. Math. 54 (2001) 1320–1342.

[29] I. Kiss, Z. Neufeld, J.H. Merkin, S.K. Scott, Combustion initiation and extinction in a two-dimensional chaotic flow, submitted for publication.

[30] W.E. Ranz, Applications of a stretch model to mixing, diffusion, and reaction in laminar and turbulent flows, AIChE J. 25 (1979) 41–47.

[31] L.J. Slater, Confluent Hypergeometric Functions, Cambridge University Press, Cambridge, 1960.